

Chapter 3

Wind Turbine Generation Systems Modeling for Integration in Power Systems

Adrià Junyent-Ferré^{*,‡} and Oriol Gomis-Bellmunt[†]

**Centre d'Innovació Tecnològica en Convertidors
Estàtics i Accionaments (CITCEA-UPC),
Departament d'Enginyeria Elèctrica,
Universitat Politècnica de Catalunya,
ETS d'Enginyeria Industrial de Barcelona,
Av. Diagonal, 647, Pl. 2. 08028 Barcelona, Spain*

*†IREC Catalonia Institute for Energy Research,
Josep Pla, B2, Pl. Baixa. E-08019 Barcelona, Spain*

‡adria.junyent@citcea.upc.edu

This chapter deals with the modeling of wind turbine generation systems for integration in power systems studies. The modeling of the wind phenomenon, the turbine mechanical system and the electrical machine, along with the corresponding converter and electrical grid is described.

3.1 Introduction

Wind power generation has grown in the last three decades and is considered one of the most promising renewable energy sources. However, its integration into power systems has a number of technical challenges concerning security of supply, in terms of reliability, availability and power quality.

Wind power impact mainly depends on its penetration level, but depends also on the power system size, the mix of generation capacity, the degree of interconnections to other systems and load variations. Since the penetration of wind power generation is growing, system operators have an increasing interest in analyzing the impact of wind power on the connected power system. For this reason, grid connection requirements are established. In the last few years, the connection requirements have incorporated, in addition to steady state problems, dynamic requirements, like voltage dip ride-through capability. This leads to the need for detailed modeling

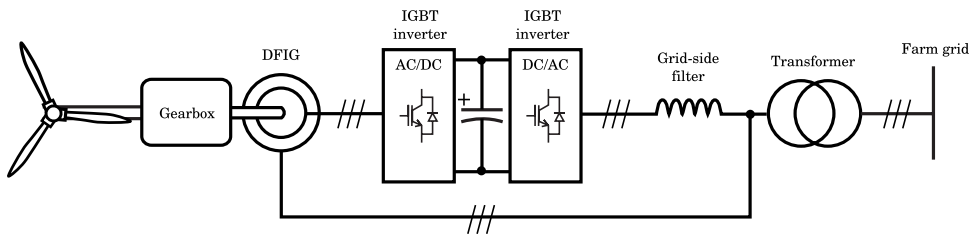


Fig. 3.1. The DFIG wind generator concept.

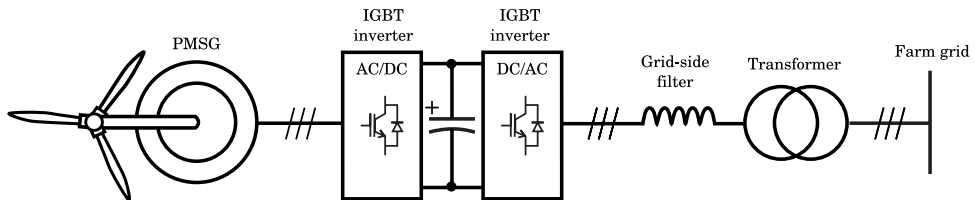


Fig. 3.2. The gearless PMSG wind generator concept.

of wind turbine systems in order to analyze the dynamic phenomena in the power grid.

Moreover, new wind turbine technology integrates power electronics and control making it possible for wind power generation to participate in active and reactive power control. Nowadays most of the installed variable speed wind generators are based on the doubly-fed induction generator (DFIG) but new types of wind generators based on permanent magnet synchronous generators (PMSG) are expected to gain market popularity in the following years. The DFIG configuration consists of a wound rotor induction generator with the stator windings directly connected to the grid and the rotor windings connected to a voltage-source back-to-back power converter which transfers a fraction of the extracted power (see Fig. 3.1). The PMSG configuration needs a full power converter and allows the use of multipolar generators making it possible to suppress the gearbox (see Fig. 3.2).

In this chapter we discuss a model for the induction and synchronous type generators, the back-to-back converter and the electrical network. Including the detailed description of the reactive power, DC bus voltage and torque controllers, along with its corresponding current loops, simulation results are analyzed and discussed.

3.2 Wind Turbine Modeling

Wind turbine electrical generation systems' power comes from the kinetic energy of the wind, thus it can be expressed as the kinetic power available in the stream of

air multiplied by a C_P factor called power coefficient. C_P mainly depends on the relation between the average speed of the air across the area covered by the wind wheel and its angular speed and geometric characteristics of the turbine (including the instantaneous blade pitch angle configuration).¹ The power extracted by the wind turbine has the following expression:

$$P_{ww} = c_P P_{\text{wind}} = c_P \frac{1}{2} \rho A v_w^3, \quad (3.1)$$

where P_{wind} is kinetic power of the air stream that crosses the turbine rotor area, ρ is the air density assumed to be constant, A is the surface covered by the turbine and v_w is the average wind speed.

There have been different approaches to model the power coefficient ranging from considering it to be constant for steady state and small signal response simulations to using lookup tables with measured data. Another common approach is to use an analytic expression originated from Ref. 1 of the form:

$$c_P(\lambda, \theta_{\text{pitch}}) = c_1 \left(c_2 \frac{1}{\Lambda} - c_3 \theta_{\text{pitch}} - c_4 \theta_{\text{pitch}}^{c_5} - c_6 \right) e^{-c_7 \frac{1}{\lambda}}, \quad (3.2)$$

where λ is the so-called tip speed ratio and it is defined as:

$$\lambda \triangleq \frac{\omega_t R}{v_1} \quad (3.3)$$

and

$$\frac{1}{\Lambda} \triangleq \frac{1}{\lambda + c_8 \theta_{\text{pitch}}} - \frac{c_9}{1 + \theta_{\text{pitch}}^3}, \quad (3.4)$$

where $[c_1 \dots c_9]$ are characteristic constants for each wind turbine and θ_{pitch} is the blade pitch angle.

Thus by knowing the wind speed, the angular speed of the wind turbine and the blade pitch angle, the mechanical torque on the turbine shaft can be easily computed:

$$\Gamma_t = c_P(v_w, \omega_t) \frac{1}{2} \rho A v_w^3, \quad (3.5)$$

where Γ_t is the turbine torque.

3.3 Wind Modeling

Wind speed usually varies from one location to another and also fluctuates over the time in a stochastic way. As it has been previously seen, it maintains a direct relation to the torque over the turbine axis and therefore it may also have some direct effect on the power output of the wind turbine generation system (WTGS) hence its evolution must be taken into account to properly simulate the WTGS dynamics.

One possible approach to generate the wind speed signal on simulations may be to use logs of real measurements of the speed on the real location of the WTGS. This approach has some evident limitations because it requires a measurement to be done on each place to be simulated. Another choice, proposed by Ref. 2 is to use a mathematical model which takes some landscape parameters to generate a wind speed sequence for any location. This wind speed expression has the form:

$$v_w(t) = v_{wa}(t) + v_{wr}(t) + v_{wg}(t) + v_{wt}(t), \quad (3.6)$$

where $v_{wa}(t)$ is a constant component, $v_{wr}(t)$ is a common ramp component, v_{wg} is a gust component and v_{wt} is a turbulence component.

The gust component may be useful to simulate an abnormal temporary increase of the speed of the wind and its expression is:

$$v_{wg}(t) = \begin{cases} 0, & \text{for } t < T_{sg} \\ \hat{A}_g \left(1 - \cos \left[2\pi \left(\frac{t - T_{sg}}{T_{eg} - T_{sg}} \right) \right] \right), & \text{for } T_{sg} \leq t \leq T_{eg} \\ 0, & \text{for } T_{eg} < t \end{cases} \quad (3.7)$$

where A_g is the amplitude of the gust and T_{sg} and T_{eg} are the start and the end time of the gust.

Finally, as discussed in Ref. 3, the turbulence component is a signal which has a power spectral density of the form:

$$P_{Dt}(f) = \frac{l\hat{v}_w \left[\ln \left(\frac{h}{z_0} \right) \right]^{-2}}{\left[1 + 1.5 \frac{fl}{\hat{v}} \right]^{5/3}}, \quad (3.8)$$

where \hat{v}_w is the average wind speed, h is the height of interest (the wind wheel height), l is the turbulence scale which is twenty times h and has a maximum of 300 m and z_0 is a roughness length parameter which depends on the landscape type as shown in Table 3.1

Table 3.1. Values of the z_0 for different types of landscapes.

Landscape type	Range of z_0 (m)
Open sea or sand	0.0001–0.001
Snow surface	0.001–0.005
Mown grass or steppe	0.001–0.01
Long grass or rocky ground	0.04–0.1
Forests, cities and hilly areas	1–5

Source: Panofsky and Dutton, 1984; Simiu and Scanlan, 1986.

By knowing the height of the wind turbine, the average wind speed and the kind of landscape where the WTGS is, the power spectral density of the wind speed turbulence is known. The next step is to generate a signal, function of time, which has the desired power spectral density. There are many ways of doing this. One approach suggested in Ref. 4 is to sum a large number of sines with random initial phase and amplitude according to the P_{Dr} . The suggested method here is to use a linear filter designed to shape a noise signal to give it the desired spectral density. Provided that the P_{Dr} is very close to the response of a first order filter, a possible filter that accomplishes this goal is:

$$H(s) = \frac{K}{s + p}, \tag{3.9}$$

where

$$p = \frac{2\pi \left((K_1^2)^{3/5} - 1 \right)}{K_2 \sqrt{K_1^2 - 1}}, \quad K = K_1 p. \tag{3.10}$$

3.4 Mechanical Transmission Modeling

The drive-train of a WTGS comprises the wind wheel, the turbine shaft, the gearbox and the generator's rotor shaft. The gearbox usually has a multiplication ratio between 50 and 150 and the wind wheel inertia usually is about the 90% of the inertia of the whole system.

Because of the high torque applied to the turbine shaft, its deformation must not be neglected and its elastic behavior should be taken into account because of its filtering properties. A common way to model the drive-train is to treat it as a series of masses connected through an elastic coupling with a linear stiffness, a damping ratio and a multiplication ratio between them. On this paper a model with two masses,

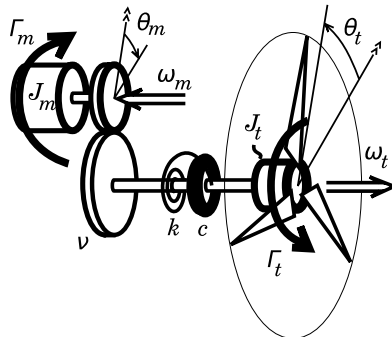


Fig. 3.3. Two mass drive-train model.

graphically presented in Fig. 3.3, is used treating the wind wheel as one inertia J_t and the gearbox and the generator's rotor as another inertia J_m connected through the elastic turbine shaft with a k angular stiffness coefficient and a c angular damping coefficient. Applying the Newton's laws, the dynamics of the resulting system can be described as:

$$\begin{bmatrix} \dot{\omega}_m \\ \dot{\omega}_t \\ \omega_m \\ \omega_t \end{bmatrix} = \begin{bmatrix} \frac{-v^2 c}{J_m} & \frac{vc}{J_m} & \frac{-v^2 k}{J_m} & \frac{vk}{J_m} \\ \frac{vc}{J_t} & -\frac{c}{J_t} & \frac{vk}{J_t} & -\frac{k}{J_t} \\ 1 & 0 & 0 & 0 \\ 0 & 1 & 0 & 0 \end{bmatrix} \begin{bmatrix} \omega_m \\ \omega_t \\ \theta_m \\ \theta_t \end{bmatrix} + \begin{bmatrix} \frac{1}{J_m} & 0 \\ 0 & \frac{1}{J_t} \\ 0 & 0 \\ 0 & 0 \end{bmatrix} \begin{bmatrix} \tau_m \\ \tau_t \end{bmatrix}, \quad (3.11)$$

where θ_t and θ_m are the angles of the wind wheel and the generator shaft, ω_t and ω_m are the angular speed of the wind wheel and the generator, τ_t is the torque applied to the turbine axis by the wind wheel and τ_m is the generator torque.

3.5 Electrical Generator Modeling

3.5.1 Induction machine

The generator of a doubly-fed WTGS is a wounded rotor asynchronous machine. We will assume the stator and rotor windings to be placed sinusoidally and symmetrical and the magnetical saturation effects and the capacitance of all the windings neglectable. Taking as positive the currents flowing towards the machine, the relations between the voltages on the machine windings and the currents and its first derivative can be written as:

$$v_s^{abc} = r_s i_s^{abc} + \frac{d}{dt} \lambda_s^{abc}, \quad (3.12)$$

$$v_r^{abc} = r_r i_r^{abc} + \frac{d}{dt} \lambda_r^{abc}, \quad (3.13)$$

where v_s^{abc} and i_s^{abc} is the stator abc voltage and current vectors, v_r^{abc} and i_r^{abc} is the rotor abc voltage and current vector, λ_s^{abc} and λ_r^{abc} are the stator and rotor flux linkage abc vectors defined as:

$$\begin{bmatrix} \lambda_s^{abc} \\ \lambda_r^{abc} \end{bmatrix} = \begin{bmatrix} L_{ss}^{abc} & L_{sr}^{abc} \\ L_{rs}^{abc} & L_{rr}^{abc} \end{bmatrix} \begin{bmatrix} i_s^{abc} \\ i_r^{abc} \end{bmatrix}, \quad (3.14)$$

where

$$L_{ss}^{abc} = \begin{bmatrix} L_{ls} + L_{ms} & -\frac{1}{2}L_{ms} & -\frac{1}{2}L_{ms} \\ -\frac{1}{2}L_{ms} & L_{ls} + L_{ms} & -\frac{1}{2}L_{ms} \\ -\frac{1}{2}L_{ms} & -\frac{1}{2}L_{ms} & L_{ls} + L_{ms} \end{bmatrix}, \quad (3.15)$$

$$L_{rr}^{abc} = \begin{bmatrix} L_{lr} + L_{mr} & -\frac{1}{2}L_{mr} & -\frac{1}{2}L_{mr} \\ -\frac{1}{2}L_{mr} & L_{lr} + L_{mr} & -\frac{1}{2}L_{mr} \\ -\frac{1}{2}L_{mr} & -\frac{1}{2}L_{mr} & L_{lr} + L_{mr} \end{bmatrix}, \quad (3.16)$$

$$L_{sr}^{abc} = \{L_{rs}^{abc}\}^t = L_{sr} \begin{bmatrix} \cos(\theta_r) & \cos(\theta_r + \frac{2\pi}{3}) & \cos(\theta_r - \frac{2\pi}{3}) \\ \cos(\theta_r - \frac{2\pi}{3}) & \cos(\theta_r) & \cos(\theta_r + \frac{2\pi}{3}) \\ \cos(\theta_r + \frac{2\pi}{3}) & \cos(\theta_r - \frac{2\pi}{3}) & \cos(\theta_r) \end{bmatrix}, \quad (3.17)$$

also, the mechanical torque can be written as a function of the machine current as:

$$\Gamma_m = \frac{P}{2} \begin{bmatrix} i_s^{abc} \\ i_r^{abc} \end{bmatrix}^t \begin{bmatrix} 0 & N_{sr}^{abc} \\ N_{rs}^{abc} & 0 \end{bmatrix} \begin{bmatrix} i_s^{abc} \\ i_r^{abc} \end{bmatrix}, \quad (3.18)$$

where

$$N_{sr}^{abc} = \{N_{rs}^{abc}\}^t = -L_{sr} \begin{bmatrix} \sin(\theta_r) & \sin(\theta_r + \frac{2\pi}{3}) & \sin(\theta_r - \frac{2\pi}{3}) \\ \sin(\theta_r - \frac{2\pi}{3}) & \sin(\theta_r) & \sin(\theta_r + \frac{2\pi}{3}) \\ \sin(\theta_r + \frac{2\pi}{3}) & \sin(\theta_r - \frac{2\pi}{3}) & \sin(\theta_r) \end{bmatrix} \quad (3.19)$$

for further details on the formulation of the voltage equations of the asynchronous machine, the reader is referred to Ref. 5.

As these equations have a hard dependency on the rotor angle position, it is not recommended its use in simulation. Instead, it is preferred to introduce the Park variable transformation to the equations and use the transformed variables to integrate the dynamical equations of the machine. The Park transformation matrix is a non-singular matrix defined as:

$$T(\theta) = \frac{2}{3} \begin{bmatrix} \cos(\theta) & \cos(\theta - \frac{2\pi}{3}) & \cos(\theta + \frac{2\pi}{3}) \\ \sin(\theta) & \sin(\theta - \frac{2\pi}{3}) & \sin(\theta + \frac{2\pi}{3}) \\ \frac{1}{2} & \frac{1}{2} & \frac{1}{2} \end{bmatrix}, \quad (3.20)$$

where θ is the so called Park reference angle which may be chosen as constant or linear time-varying for different purposes.

The $qd0$ transformed variables are defined as:

$$x^{qd0} \equiv T(\theta)x^{abc}. \quad (3.21)$$

By choosing $\theta = \omega_s t$ where ω_s is the nominal grid frequency for the stator variables transformation and $\theta = \omega_s t - \theta_r$ where θ_r is the rotor angular position multiplied by the number of pole pairs of the machine for the rotor variables, the machine current and voltage variables written in qd become constant in steady state, which benefits the numerical integration methods used by the simulation software.

By doing this, the machine equations can be written as:

$$\begin{bmatrix} v_{sq} \\ v_{sd} \\ v_{rq} \\ v_{rd} \end{bmatrix} = \begin{bmatrix} L_s & 0 & M & 0 \\ 0 & L_s & 0 & M \\ M & 0 & L_r & 0 \\ 0 & M & 0 & L_r \end{bmatrix} \frac{d}{dt} \begin{bmatrix} i_{sq} \\ i_{sd} \\ i_{rq} \\ i_{rd} \end{bmatrix} + \begin{bmatrix} r_s & L_s \omega_s & 0 & M \omega_s \\ -L_s \omega_s & r_s & -M \omega_s & 0 \\ 0 & sM \omega_s & r_r & sL_r \omega_s \\ -sM \omega_s & 0 & -sL_r \omega_s & r_r \end{bmatrix} \begin{bmatrix} i_{sq} \\ i_{sd} \\ i_{rq} \\ i_{rd} \end{bmatrix} \quad (3.22)$$

and

$$V_{s0} = L_{ls} \frac{di_{s0}}{dt} + r_s i_{s0}, \quad (3.23)$$

$$V_{r0} = L_{lr} \frac{di_{r0}}{dt} + r_r i_{r0}, \quad (3.24)$$

where $L_s \equiv \frac{3}{2}L_{ms} + L_{ls}$ and $L_r \equiv \frac{3}{2}L_{mr} + L_{lr}$ are the stator and rotor windings self-inductance coefficient, $M = \frac{3}{2}L_{sr}$ is the coupling coefficient between stator and rotor windings and s is the slip defined as the relation between the mechanical speed and the reference frame angular speed ($s \triangleq \frac{\omega_s - \omega_r}{\omega_s}$).

Also the torque expression and the stator reactive power, which are the control objectives of the rotor-side converter control, have the following form:

$$\Gamma_m = \frac{3}{2}PM(i_{sq}i_{rd} - i_{sd}i_{rq}), \quad (3.25)$$

where P is the number of pairs of poles of the generator.

Also, according to the so-known *pq-theory*⁶ the instantaneous reactive power can be written as:

$$Q_s = \frac{3}{2}(v_{sq}i_{sd} - v_{sd}i_{sq}). \quad (3.26)$$

3.5.2 Permanent magnet synchronous machine

To model the dynamical behavior of the permanent magnet synchronous machine, we will assume again the stator windings to be placed sinusoidally and symmetrical and the magnetical saturation effects and the capacitance of all the windings neglectable. Taking as positive the currents flowing towards the machine, the relations between the voltages on the machine windings and the currents and its first derivatives can be written as⁷:

$$v_s^{abc} = r_s i_s^{abc} + \frac{d}{dt} \lambda_s^{abc}, \quad (3.27)$$

where the stator flux linkage in abc can be written as:

$$\lambda_s^{abc} = ([L_1] + [L_2(\theta_r)]) i_s^{abc} + \lambda_m \begin{bmatrix} \sin(\theta_r) \\ \sin(\theta_r - \frac{2\pi}{3}) \\ \sin(\theta_r + \frac{2\pi}{3}) \end{bmatrix} \quad (3.28)$$

and

$$[L_1] = \begin{bmatrix} L_{ls} + L_A & -\frac{1}{2}L_A & -\frac{1}{2}L_A \\ -\frac{1}{2}L_A & L_{ls} + L_A & -\frac{1}{2}L_A \\ -\frac{1}{2}L_A & -\frac{1}{2}L_A & L_{ls} + L_A \end{bmatrix}, \quad (3.29)$$

$$[L_2(\theta_r)] = -L_B \begin{bmatrix} \cos 2(\theta_r) & \cos 2(\theta_r - \frac{\pi}{3}) & \cos 2(\theta_r + \frac{\pi}{3}) \\ \cos 2(\theta_r - \frac{\pi}{3}) & \cos 2(\theta_r + \frac{\pi}{3}) & \cos 2(\theta_r) \\ \cos 2(\theta_r + \frac{\pi}{3}) & \cos 2(\theta_r) & \cos 2(\theta_r - \frac{\pi}{3}) \end{bmatrix}, \quad (3.30)$$

where λ_m is the flux due to the rotor magnet, L_A is the constant fraction of the stator linkage inductance and L_B is a rotor position dependent inductance term due to rotor asymmetry.

The mechanical torque can be written as:

$$\Gamma_m = P \left(\{i_s^{abc}\}^T \frac{d}{d\theta_r} [L_2(\theta_r)] i_s^{abc} + \lambda_m \{i_s^{abc}\}^T \begin{bmatrix} \cos(\theta_r) \\ \cos(\theta_r - \frac{2\pi}{3}) \\ \cos(\theta_r + \frac{2\pi}{3}) \end{bmatrix} \right). \quad (3.31)$$

By differentiating the stator flux linkage variables over time, we get:

$$\begin{aligned} \frac{d}{dt} \lambda_s^{abc} &= ([L_1] + [L_2(\theta_r)]) \frac{d}{dt} i_s^{abc} + \omega_r \frac{d}{d\theta_r} [L_2(\theta_r)] i_s^{abc} \\ &\quad + \lambda_m \omega_r \begin{bmatrix} \cos(\theta_r) \\ \cos(\theta_r - \frac{2\pi}{3}) \\ \cos(\theta_r + \frac{2\pi}{3}) \end{bmatrix}. \end{aligned} \quad (3.32)$$

By substituting the flux linkage expression in the Eq. (3.27), the explicit relation between current and voltage is obtained:

$$\begin{aligned} v_s^{abc} &= \left(r_s [I_3] + \omega_r \frac{d}{d\theta_r} [L_2(\theta_r)] \right) i_s^{abc} + ([L_1] + [L_2(\theta_r)]) \frac{d}{dt} i_s^{abc} \\ &\quad + \lambda_m \omega_r \begin{bmatrix} \cos(\theta_r) \\ \cos(\theta_r - \frac{2\pi}{3}) \\ \cos(\theta_r + \frac{2\pi}{3}) \end{bmatrix}. \end{aligned} \quad (3.33)$$

As in the case of the induction machine, we see a strong dependency on the rotor position which is not desirable for the numerical stability of the integration algorithm used in simulation. We introduce a Park variable transformation for the stator variables taking $\theta = \theta_r$ which gives constant values to the voltage and current variables in steady state. The system equations in this reference frame can be written as:

$$v_s^{qd} = \begin{bmatrix} r_s & \omega_r (L_{ls} + \frac{3}{2} (L_A + L_B)) \\ -\omega_r (L_{ls} + \frac{3}{2} (L_A - L_B)) & r_s \end{bmatrix} i_s^{qd} + \begin{bmatrix} L_{ls} + \frac{3}{2} (L_A - L_B) & 0 \\ 0 & L_{ls} + \frac{3}{2} (L_A + L_B) \end{bmatrix} \frac{d}{dt} i_s^{qd} + \lambda_m \omega_r \begin{bmatrix} 1 \\ 0 \end{bmatrix} \quad (3.34)$$

and

$$v_s^0 = r_s i_s^0 + L_{ls} \frac{d}{dt} i_s^0, \quad (3.35)$$

also the torque can be rewritten as:

$$\Gamma_m = \frac{3}{2} P \left(\left\{ i_s^{qd0} \right\}^T \begin{bmatrix} 0 & 3L_B & 0 \\ 3L_B & 0 & 0 \\ 0 & 0 & 0 \end{bmatrix} i_s^{qd0} + \lambda_m \left\{ i_s^{qd0} \right\}^T \begin{bmatrix} 1 \\ 0 \\ 0 \end{bmatrix} \right). \quad (3.36)$$

3.6 Converter Modeling

The most common converter topology used in variable speed wind turbines is the forced commutation voltage source back-to-back converter with insulated-gate bipolar transistors (IGBT). The structure of this type of converter is shown in Fig. 3.4. The AC side on the left, which we will call the machine side, is connected to the rotor of the machine in the DFIG configuration and to the stator of the machine in the PMSG while the right AC side, grid side from now on, is connected to the wind turbine transformer (see also Figs. 3.1 and 3.2). Notice that the current direction is depicted according to the machine equations discussed in the previous section.

The dynamics of the converter involve continuous state variables corresponding to voltages and currents and discrete states corresponding to the commutation state of the IGBTs. These dynamics are complex to model and simulate and different levels of detail may be achieved by doing some assumptions. Usually an averaged converter model is used, neglecting the commutation effects assuming they are filtered by the low-pass dynamics of the rest of the system.

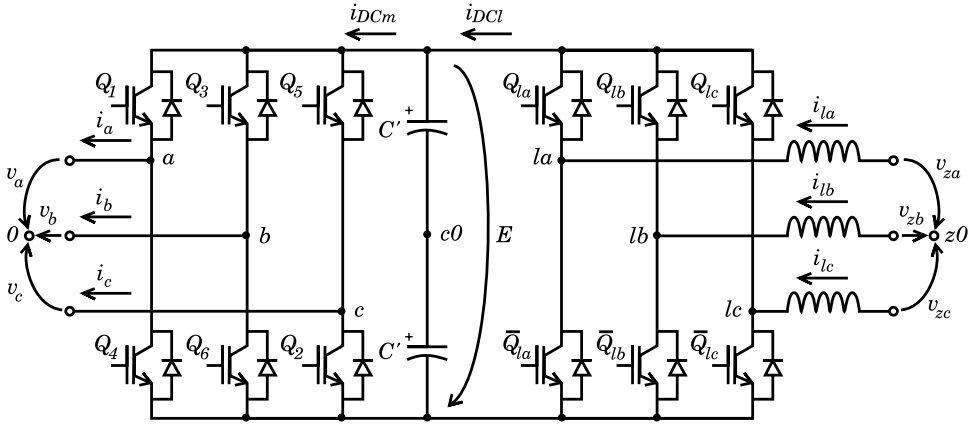


Fig. 3.4. The IGBT voltage source back-to-back converter.

Making this assumptions, the dynamics of the grid-side electrical circuit between the grid voltage and the voltage applied on the AC side of the converter assuming the currents are positive when flowing towards the machine can be described as:

$$v_z^{abc} - v_l^{abc} - (v_{c0} - v_{z0}) \begin{bmatrix} 1 \\ 1 \\ 1 \end{bmatrix} = r_l i_l^{abc} + L_l \frac{d}{dt} i_l^{abc}, \quad (3.37)$$

also when no neutral conductor is present, it can be stated that:

$$v_{c0} - v_{z0} = \frac{1}{3} [1 \ 1 \ 1] \cdot (v_z^{abc} - v_l^{abc}), \quad (3.38)$$

where v_z^{abc} and v_l^{abc} are the abc voltages on the grid side of the grid converter filter and the AC side of the converter, r_l is the resistance of the filter inductors and L_l is the inductance of the filter.

The dynamics of the voltage of the DC bus can be described as:

$$\frac{dE}{dt} = \frac{1}{C} (i_{DCl} - i_{DCm}), \quad (3.39)$$

where E is the voltage of the DC bus, i_{DCl} is the current through the DC side of the grid-side inverter, i_{DCm} is the current through the machine side inverter and both currents can be computed by doing a power balance on each inverter:

$$E i_{DCm} = v_a i_a + v_b i_b + v_c i_c, \quad (3.40)$$

$$E i_{DCl} = v_{la} i_{la} + v_{lb} i_{lb} + v_{lc} i_{lc}. \quad (3.41)$$

3.7 Control Modeling

In this section the control of the wind turbine is briefly explained. First we introduce a simple speed control that gives the torque reference that the generator must follow. Then the basics of the electrical control of the DFIG, the PMSG and the grid side converter are presented.

3.7.1 Speed control

The purpose of the speed controller is to maximize the power extracted by the turbine. The power available in the wind is a function of the wind speed thus extracting the maximum power available would require, at least, knowing exactly the value of the wind speed. To avoid the dependency on wind speed measurements, a series of open-loop control algorithms have been developed, the most common of them being the constant tip speed ratio control.⁸ This control scheme is based on the fact that given a fixed wind speed, it can be proved that the optimal operation point can be achieved by controlling the generator so that the torque follows a function of the square of the wind speed. This function can be expressed as:

$$\Gamma_m^* = \frac{1}{v} K_{C_p} \omega_t^2, \quad (3.42)$$

where Γ_m^* is the desired generator torque and K_{C_p} is a parameter which depends on the characteristics of the turbine:

$$K_{C_p} = \frac{1}{2} \rho A R^3 \frac{c_1 (c_2 c_7 c_9 + c_6 c_7 + c_2)^3 e^{-\frac{c_6 c_7 + c_2}{c_2}}}{c_2^2 c_7^4}. \quad (3.43)$$

3.7.2 DFIG current dynamics decoupling and linearization

DFIG is controlled by applying voltages to the rotor of the machine in order to obtain the desired rotor currents. The desired rotor current values can be calculated given a grid voltage and the desired torque and stator reactive power values in steady state. From the equations of the DFIG machine we see that:

$$i_{rq}^* = -\frac{2L_s}{3PMv_{sq}} \Gamma_m^*, \quad (3.44)$$

$$i_{rd}^* = -\frac{2L_s}{3Mv_{sq}} Q_s^* + \frac{v_{sq}}{\omega_e M}, \quad (3.45)$$

where i_{rq}^* and i_{rd}^* are the rotor current reference values and Γ_m^* and Q_s^* are the desired torque and reactive power.

To be able to design a current controller a linearization and decoupling feedback is introduced:

$$\begin{bmatrix} v_{rq} \\ v_{rd} \end{bmatrix} = \begin{bmatrix} \hat{v}_{rq} + s\omega_s (Mi_{sd} + L_r i_{rd}) \\ \hat{v}_{rq} - s\omega_s (Mi_{sq} + L_r i_{rq}) \end{bmatrix}, \quad (3.46)$$

where \hat{v}_{rq} and \hat{v}_{rd} are the new auxiliary voltage inputs.

This way the voltage-current relations of the resulting system become equivalent to a circuit with a resistor in series with an inductor:

$$\begin{bmatrix} i_{rq}(s) \\ i_{rd}(s) \end{bmatrix} = \begin{bmatrix} \frac{1}{L_r s + r_r} & 0 \\ 0 & \frac{1}{L_r s + r_r} \end{bmatrix} \begin{bmatrix} \hat{v}_{rq}(s) \\ \hat{v}_{rd}(s) \end{bmatrix}. \quad (3.47)$$

3.7.3 PMSG current dynamics decoupling and linearization

PMSG is controlled by applying voltages to the stator of the machine to obtain the desired stator current evolution. As in the DFIG, the stator current reference values can be calculated to obtain the desired steady state torque and to achieve different objectives like minimizing the stator current or obtaining the maximum torque with a given stator voltage modulus. From the steady state equations of the PMSG we see that to control the desired torque we need:

$$i_{sq}^* = -\frac{2}{3P\lambda_m} \Gamma_m^*. \quad (3.48)$$

Also to simplify the design of the current controllers, we introduce a linearization and decoupling feedback⁹:

$$\begin{bmatrix} v_{sq} \\ v_{sd} \end{bmatrix} = \begin{bmatrix} \hat{v}_{sq} + \omega_r (L_{ls} + \frac{3}{2} (L_A + L_B)) i_{sd} + \omega_r \lambda_m \\ \hat{v}_{sq} - \omega_r (L_{ls} + \frac{3}{2} (L_A - L_B)) i_{sq} \end{bmatrix}, \quad (3.49)$$

where \hat{v}_{sq} and \hat{v}_{sd} are the new auxiliary voltage inputs.

This way the voltage-current relations of the resulting system become:

$$\begin{bmatrix} i_{sq}(s) \\ i_{sd}(s) \end{bmatrix} = \begin{bmatrix} \frac{1}{(L_{ls} + \frac{3}{2} (L_A - L_B))s + r_s} & 0 \\ 0 & \frac{1}{(L_{ls} + \frac{3}{2} (L_A + L_B))s + r_s} \end{bmatrix} \begin{bmatrix} \hat{v}_{sq}(s) \\ \hat{v}_{sd}(s) \end{bmatrix}. \quad (3.50)$$

3.7.4 Grid-side converter control

The goal of the grid side converter control is to maintain the DC bus voltage in the desired nominal value and also to produce the desired reactive power through the grid side converter. Taking the v_z grid voltage angle as the reference angle it can

be seen that the output reactive power is proportional to i_{ld} while the active power is proportional to i_{lq} . Thus, from the steady state equations, a reference value can be deduced for i_{ld} to obtain the desired reactive power:

$$i_{ld}^* = \frac{2}{3v_{zq}} Q_z^* \quad (3.51)$$

The DC bus regulation is done through i_{lq} by feeding the voltage error to a proportional-integrator (PI) controller to obtain a 0 voltage steady state error:

$$i_{lq}^* = \frac{K_p s + K_i}{s} (E^* - E). \quad (3.52)$$

Given the current reference values, current controllers can be designed with ease introducing the following linearization and decoupling feedback:

$$\begin{bmatrix} v_{lq} \\ v_{ld} \end{bmatrix} = \begin{bmatrix} \hat{v}_{lq} + \omega_s L_l i_{ld} + v_{zq} \\ \hat{v}_{lq} - \omega_s L_l i_{lq} \end{bmatrix}, \quad (3.53)$$

where \hat{v}_{lq} and \hat{v}_{ld} are the new auxiliary voltage inputs.

This way the voltage-current relations of the resulting system become:

$$\begin{bmatrix} i_{lq}(s) \\ i_{ld}(s) \end{bmatrix} = \begin{bmatrix} \frac{1}{L_l s + r_l} & 0 \\ 0 & \frac{1}{L_l s + r_l} \end{bmatrix} \begin{bmatrix} \hat{v}_{lq}(s) \\ \hat{v}_{ld}(s) \end{bmatrix}. \quad (3.54)$$

3.7.5 Current controller design

We have shown that for each system, we can introduce a linearization and decoupling feedback from measured magnitudes and transform a multivariable system with time-varying parameters into a circuit with a resistor in series with an inductor. Thus the same current controller design procedure can be applied to each system. Here we briefly present a PI design for a RL circuit.

For a given RL circuit, the current dynamics can be expressed in the Laplace domain as a function of the applied voltages as:

$$i(s) = \frac{1}{Ls + r} v(s). \quad (3.55)$$

This corresponds to a first order system, hence it can be controlled with a PI controller achieving a zero steady state error and a desired closed loop settling time. This controller can be expressed as

$$v(s) = \frac{K_i + K_p s}{s} (i^*(s) - i(s)) \quad (3.56)$$

and

$$K_p = \frac{L}{\tau}, \quad K_i = \frac{r}{\tau}, \quad (3.57)$$

where K_p and K_i are the proportional and integral parameters of the PI controller and τ is the desired closed loop time constant.¹⁰

The closed loop transfer function of the current as a function of the current reference becomes:

$$i(s) = \frac{1}{\tau s + 1} i^*(s). \quad (3.58)$$

3.8 Electrical Disturbances

We introduce here a general three phase grid voltage expression:

$$v_z^{abc}(t) = \frac{\sqrt{2}}{\sqrt{3}} V_D(t) \begin{bmatrix} \cos(\varphi_D(t)) \\ \cos(\varphi_D(t) - \frac{2\phi}{3}) \\ \cos(\varphi_D(t) + \frac{2\phi}{3}) \end{bmatrix} + \frac{\sqrt{2}}{\sqrt{3}} V_I(t) \begin{bmatrix} \cos(\varphi_I(t)) \\ \cos(\varphi_I(t) + \frac{2\phi}{3}) \\ \cos(\varphi_I(t) - \frac{2\phi}{3}) \end{bmatrix} \quad (3.59)$$

and

$$\varphi_D(t) = \varphi_D(0) + \int_0^t \omega_s(t) dt, \quad (3.60)$$

$$\varphi_I(t) = \varphi_I(0) + \int_0^t \omega_s(t) dt, \quad (3.61)$$

where $V_D(t)$ and $V_I(t)$ are the phase-to-phase positive and negative sequence voltage rms values as functions of time, $\varphi_D(t)$ and $\varphi_I(t)$ are the phase angles of the positive and negative sequences, and $\omega_s(t)$ is the derivative of the phase angles.

The wind turbine system's response to a series of grid fault types can be simulated by inputting the right grid voltages to the presented model, the function definitions to accomplish this can be seen on Table 3.2

3.9 Conclusions

In this chapter we have presented a dynamical simulation model for the DFIG and the PMSG wind generators which are the main types of variable speed wind generators that we will see in wind farms in following years, DFIG being the most common nowadays. First we presented a wind able to simulate the evolution of its speed for a given wind turbine location. Then we have introduced a simple model that describes the dynamic behavior of the wind turbine mechanical components and the generator electrical dynamics. Finally we have briefly discussed the control of both

Table 3.2. Grid voltage function definition for different grid faults simulation.

Fault type	Function	Value	Comments
Symmetrical voltage sag	$V_D(t)$	$V^N (1 - \alpha u(t - t_0))$	V_N is the nominal voltage, α is the per-unit dip amplitude, $u(t - t_0)$ is a t_0 delayed step function
	$V_I(t)$	0	
	$\omega_s(t)$	ω_s^N	ω_s^N is the nominal grid frequency
Asymmetrical voltage sag	$V_D(t)$	$V^N (1 - \alpha_D u(t - t_0))$	α is the per-unit positive sequence dip amplitude
	$V_I(t)$	$V_I u(t - t_0)$	V_I is the negative sequence amplitude during the asymmetrical dip
	$\omega_s(t)$	ω_s^N	ω_s^N is the nominal grid frequency
Frequency step change	$V_D(t)$	V^N	
	$V_I(t)$	0	
	$\omega_s(s)$	$\omega_s^N (1 + \alpha_\omega)$	α_ω is the per-unit grid frequency increase

wind turbine topologies and how we can model a series of electrical disturbances of interest with the model.

References

1. S. Heier, *Grid Integration of Wind Energy Conversion Systems* (John Wiley and Sons, 1998).
2. J.G. Slootweg, "Reduced-order modelling of wind turbines," in *Wind Power in Power Systems*, (Wiley, 2005), pp. 555–585.
3. H.A. Panofsky and J.A. Dutton, *Atmospheric Turbulence*. (Wiley-Interscienc, 1984).
4. M. Shinozuka and C.-M. Jan, "Digital simulation of random processes and its applications," *J. Sound and Vibration* **25** (1972) 111–128.
5. P.C. Krause, *Analysis of Electric Machinery* (McGraw-Hill, 1986).
6. H. Akagi, E. Watanabe and M. Aredes, *Instantaneous Power Theory and Applications to Power Conditioning* (Wiley, 2007).
7. P.D. Chandana-Perera, "Sensorless control of permanent-magnet synchronous motor drives," PhD thesis, Faculty of Engineering & Science at Aalborg University (2002).
8. D. Goodfellow and G. Smith, "Control strategy for variable speed of a fixed-pitch wind turbine operating in a wide speed range," *Proc. 8th BWEA Conf.*, Cambridge (1986), pp. 219–228.
9. M. Chinchilla, S. Arnaltes and J.C. Burgos, "Control of permanent-magnet generators applied to variable-speed wind-energy systems connected to the grid," *IEEE Trans. Energy Conversion* **21** (2006) 130–135, doi: 10.1109/TEC.2005.853735.
10. L. Harnefors and H.-P. Nee, "Model-based current control of ac machines using the internal model control method," *IEEE Trans. Industry Applications* **34** (1999) 133–141, doi: 10.1109/28.658735.